International Compressor Engineering Conference

School of Mechanical Engineering

2021

Novel Refrigeration Cycle with Continuous Cooling Turbo Compressor and Condensing Ejector Using Water as Refrigerant

Tadayoshi Shoyama
Panasonic Corporation, Japan

Bunki Kawano

Iori Maruhashi
maruhashi.iori@jp.panasonic.com

Hongzhi Sun

Michiyoshi Kusaka

See next page for additional authors

Authors

Tadayoshi Shoyama, Bunki Kawano, Iori Maruhashi, Hongzhi Sun, Michiyoshi Kusaka, Junki Yoshimoto, and Masaru Matsui

Novel Refrigeration Cycle with Continuous Cooling Turbo Compressor and Condensing Ejector Using Water as Refrigerant

Tadayoshi SHOYAMA [1,2]*, Bunki KAWANO [1], Iori MARUHASHI [1], Michiyoshi KUSAKA [1],
Hongzhi SUN [1], Junki YOSHIMOTO [1], and Masaru MATSUI [1]

[1]Panasonic Corporation, Appliances Company,
Moriguchi, Osaka 570-8501, Japan
[2]E-mail: shoyama.tadayoshi@jp.panasonic.com

* Corresponding Author

ABSTRACT

Turbo chiller using water as a refrigerant was developed. A refrigeration cycle using water (R718) as a refrigerant has a high theoretical efficiency, but the cycle pressure ratio is high, and the compressor discharge temperature is elevated. Although the conversion of the compressor to a multistage compressor and the addition of an intercooler between each stage are known to lower the discharge temperature and improve performance, the resulting increased size is problematic. To resolve this issue, this study develops a refrigeration cycle that lowers discharge temperature during the compression process without enlarging the device. Using a continuous cooling compressor that compresses refrigerant vapor while continuously cooling it in process and a condensing ejector that condenses the vapor while compressing it, we experimentally verify the performance of each element. Based on the results, we verify the basic principles of a continuous cooling compressor for continuously cooling compressed vapor with refrigerant droplets sprayed by nozzles installed on the impeller. In addition, the condensing ejector uses a high-speed fine refrigerant droplets to transfer momentum to the refrigerant vapor. And thus raises its pressure within a two-phase state and simultaneously condensing refrigerant vapor.

1. INTRODUCTION

In recent years, reduced global warming potential (GWP) has been sought after the Kigali amendment to the Montreal Protocol and the requirements of F-gas regulations. Thus, there has been a movement to switch to low-GWP refrigerants, and a lot of attention has been given to the development of natural refrigerants. Natural refrigerants include propane (R290) and ammonia (R717); however, their flammability and toxicity are a problem. On the other hand, water (R718) may be the ultimate refrigerant as it is nontoxic, inflammable, and highly stable. It is also zero rated in terms of its GWP and ozone depletion potential (ODP). Furthermore, its theoretical coefficient of performance (COP) is high (Kilicarslan and Müller, 2005). A typical chiller for a water refrigerant is an absorption chiller heater, which uses a gaseous vapor absorption cycle. Several electrical vapor compression cycle-type products are available, but these consist only of the eChiller by Efficient Energy and MizTurbo, which was developed by Kawasaki Heavy Industries. Our company has developed a water refrigerant system equipped with a two-stage turbo compressor using water both as a refrigerant and a compressor bearing lubricant, and it has achieved a COP of 5.0, which corresponds to the same efficiency as conventional refrigerants (Shoyama et al., 2020). However, due to the high cycle pressure ratio, the compressor discharge superheat is high. Therefore, we mixed refrigerant droplets into compression process refrigerant vapor to develop a novel continuous cooling turbo compressor that compresses with no superheat. We also develop a condensing ejector that compresses and condenses refrigerant vapor with no superheat using fine and high-speed refrigerant droplet spray. This paper reports on our construction of a refrigeration cycle using the above new elemental technology, and we demonstrate its principle of operation.

2. THEORY AND DESIGN

2.1 Refrigeration Cycle

Figure 1 shows the refrigeration cycle diagram of a conventional water refrigerant chiller, and Fig. 2 shows the developed refrigeration cycle. A conventional refrigeration cycle cools compressor discharge and prevents superheat using an intercooler. The continuous cooling turbo compressor constructed in this study has a three-stage compression configuration, and it achieves both miniaturization (high specific speed) and high efficiency (inlet Mach number $\leq$ 0.8). The impeller at each stage is equipped with a nozzle for spraying water using the centrifugal force of the impeller rotations, and it compresses the refrigerant vapor while cooling it with sprayed refrigerant droplets. It compresses the refrigerant vapor while removing excess heat from the compression process, thus reducing the compression power. In addition, refrigerant vapor discharged from the compressor is condensed by a heat exchanger in a conventional refrigeration cycle. In contrast, the condensing ejector consists of a nozzle and a mixing chamber, and it sprays refrigerant liquid that has had its heat dissipated with a cooling tower via a plate heat exchanger at high-speed from a nozzle within the mixing chamber. Then, it compresses refrigerant vapor discharged from the continuous cooling turbo compressor with sprayed refrigerant droplets. While in a gas–liquid two-phase state, it is then pressurized, and any excess heat in the compression process is continuously cooled, such that refrigerant vapor condenses from gas–liquid nonequilibrium (Marble, 1968). Refrigerant liquid condensed by the condensing ejector is returned to an evaporator via a two-stage economizer system. The design values of the water refrigerant chiller are a cycle pressure ratio of 7.0, continuous cooling turbo compressor pressure ratio of 5.3, condensing ejector pressure ratio of 1.3, and cycle COP of 6.0.
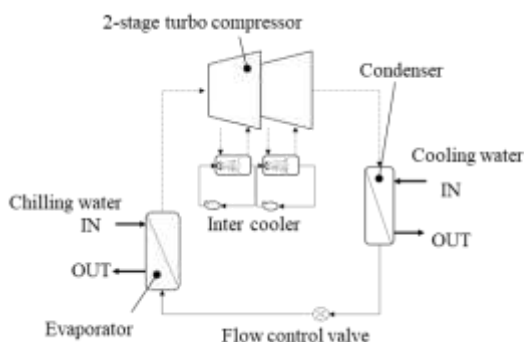

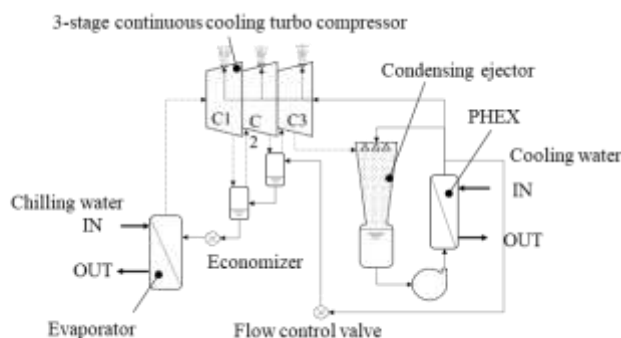**Figure 1:** Conventional refrigeration chiller.

Figure 2: Developed refrigeration chiller.

2.2 Continuous Cooling Compressor

The spraying of refrigerant droplets from the compressor inlet is known as a method of cooling and simultaneous compression using the latent heat of evaporation, and it also contributes a decrease in theoretical power (Wu, et al. 2019). However, in a water refrigerant turbo compressor in which the impeller and refrigerant droplets have a high relative velocity, blades erosion poses a problem. In the continuous cooling compression employed in this study, centrifugally pressurized spray is used. Centrifugally pressurized spray involves spraying with a nozzle embedded within a rotating impeller, as shown in Fig. 3. Using the centrifugal force of the impeller, refrigerant droplets that are fine enough to be carried by the compressed vapor flow are generated and sprayed inside the impeller. Water is supplied to the hub surface from the axial channel passing through the shaft center. A nozzle is attached to the end of the radial channel, thus pressurized water is supplied by the centrifugal action of the rotations, and is then sprayed from the nozzle. This axial channel also provides a centrifugally pressurized supply to water-lubricated bearings. The benefits of this approach are that the relative velocity of the refrigerant droplets and impeller is low, thus the erosion is suppressed, and a sufficiently high pressure is achieved from the high-speed rotations of the impeller. Providing a channel and nozzle on the impeller results in vibration problems due to increased unbalance, but these can be overcome by adjusting the nozzle placement; thus, we adopted a centrifugally pressurized spray. Below, we describe the design of the compressor.
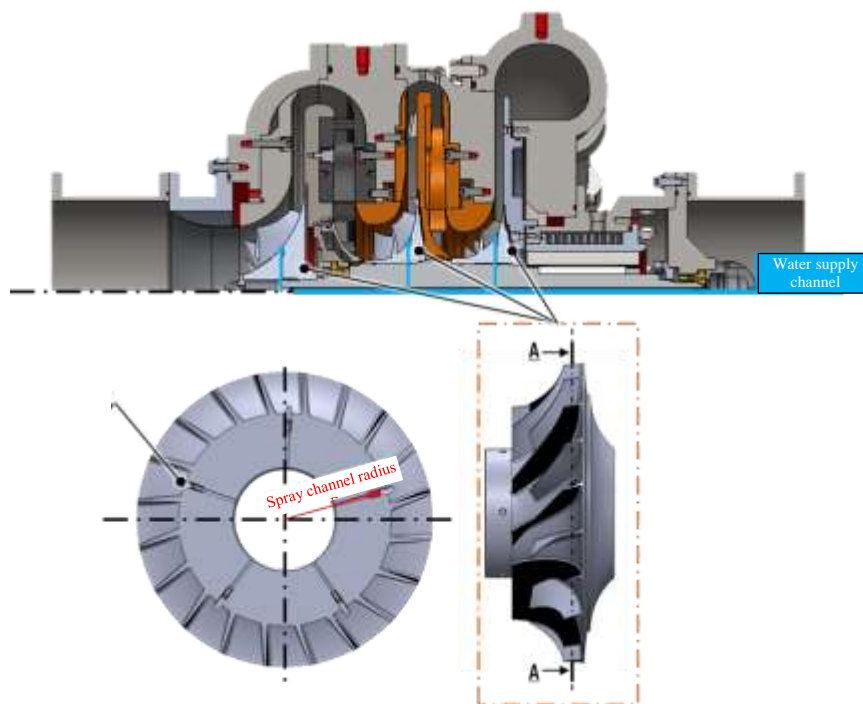
Figure 3: Cross section of the turbo compressor and its impeller.

In a previous study (Shoyama et al., 2020), a turbo compressor was developed for a water refrigerant heat pump with a 30RT refrigeration capacity, and a centrifugal impeller with a specific speed of 0.7 and an outer diameter of φ360 mm was designed. In the aerodynamic design of the impellers, the specific speed was increased to 1.4 with three stage impellers. The inlet Mach number increases, but by keeping it below 0.8, it is possible to prevent reduction of aerodynamic performance due to shock waves that may be generated at the leading edge.
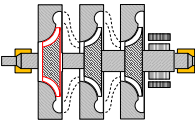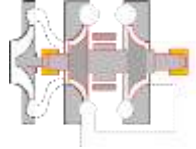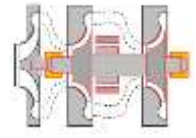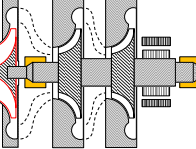
Three impellers (I), one motor (M), and two bearings (B) are arranged on the main shaft. This arrangement was necessary considering multiple factors, including the rotor dynamics of the high-speed rotor, configuration of the refrigerant channel, and assembly and disassembly work. Table 1 shows a comparison of each shaft arrangement. The BIIIMB arrangement in which bearings are arranged at both shaft ends is the same as that of the 30RT compressor that was developed. There is the benefit of being able to replace the bearing without removing the impeller; mechanical loss is also minimized because the bearing size can be reduced. However, because the first-stage impeller inlet has a bearing, the refrigerant suction area is narrow, which is a major disadvantage of the impeller miniaturization. In the IBIMIB arrangement, the thrust force can be canceled by a pair of back-to-back impellers. In addition, this configuration can be regarded as a configuration of the 30RT compressor (BIMIB arrangement) where a first-stage impeller has been added to one shaft end. Therefore, one advantage is that developing a rotation system is associated with low risk. However, because the discharge side of the impeller and the suction side of the next stage are separated, a piping is difficult to connect the discharge surface to the suction surface of the next stage. It also increases the size of the entire system.

In the same IBIMIB arrangement, when the impellers are arranged in the same direction, no piping problems exist. However, when the motor is arranged close to the middle, the middle part assumes a larger diameter for the shaft to have a higher bending natural frequency, which enlarges the motor diameter. Due to a large refrigerant vapor specific volume, the size of a motor is small relative to a conventional fluorocarbon refrigerant turbo compressor. When a large motor is arranged in the middle of the shaft, an over-engineered motor is required, which is not only high cost but has a low maximum rotation speed owing to centrifugal force limitations, making it unsuitable for the operating frequency. Consequently, it is better to arrange a motor near the shaft ends where small diameter motor can be applied.

The IBIIMB arrangement that was finally adopted satisfies the required conditions of the first-stage inlet Mach number, motor size, and pipe arrangement mentioned above. Although it poses disadvantages in terms of the bearing replacement and large thrust force, these are acceptable. The advantage is that the bending natural frequency of the

shaft is increased, thus it is possible to sufficiently separate the operating frequency range and bending resonance frequency.

Table 1: Ground design.

	BIIIMB	IBIMIB		IBIIMB
	Outboard bearing	Back-to-back impeller motor center	Same direction impeller motor center	Same direction impeller motor shaft ends
1st stage inlet area	×	○	○	○
Bearing replacement work	◎	○	○	○
Thrust force	○	◎	○	○
Motor size	○	×	×	○
Pipe arrangement	○	×	○	○
Total	×	×	×	○

For the bearing, we used a saturated water journal bearing, which has been used with a turbo compressor for the previous water refrigerant heat pump. However, because the three impellers are all facing the same direction and the thrust force is not cancel, we used a bearing in which the thrust support part and radial support part were integrated for the 1st-stage side bearing. Figure 4 shows a cross-sectional diagram of a 1st-stage side bearing. Because the thrust force of the impeller acts toward the 1st-stage side bearing, the 3rd-stage side bearing does not have to have a thrust support part. However, considering the possibility of the shaft movement to the rear-stage side due to disturbances at the start and stop, we used a tapered radial bearing. The cross-section of the bearing surface has 3-lobe shape with a preload factor of 0.6 to reduce self-excited vibration, such as whirl and whip.
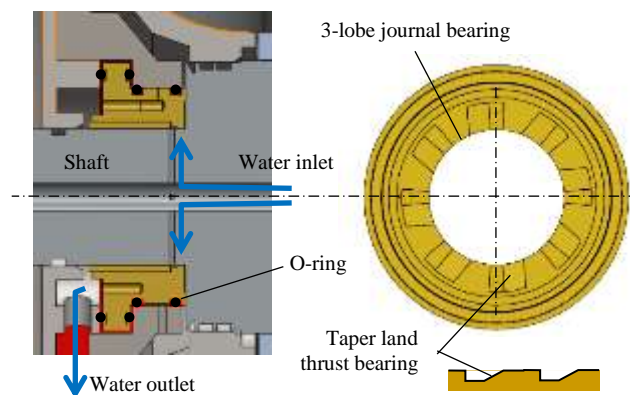

Figure 4: Water-lubricated integrated bearing.

To achieve both atomization and reduced erosion risk, we did not adopt a high-pressure atomization nozzle using an external pump for the compressor. instead, we used a centrifugal pressure nozzle built into the compressor. The

centrifugal pressure nozzle rotates at the same time as the impeller, so the relative velocity of the impeller and refrigerant droplets is small, and there is little risk of erosion of the impeller from droplet collisions. The pressure applied to the nozzle during high-speed rotations is determined by the rotational velocity and rotational radius. The pressure P applied to the nozzle is expressed as follows:

$$P = \frac{1}{2}\rho(\omega r)^2 \qquad (1)$$

Where ρ is the water density, ω is the angular rotation speed, and r is the radius with nozzle attached. In the compressor operating conditions (design values) shown in Table 2, 4.2 g/s was the calculation result obtained for the spray flow rate that is required to achieve continuous cooling compression process, under the assumption that compression process with an adiabatic efficiency of 80 %.

Table 2: Nozzle spray flow rate.

	Rotation speed, rpm	Spray radius, mm	Pressure, MPa	Spray flow rate, g/s
1st stage	24500	73.6	17.8	1.3
2nd stage	24500	85.6	24.1	1.4
3rd stage	24500	92.6	28.2	1.5

Figure 5 shows a cross-sectional diagram of a centrifugal pressure nozzle embedded in an impeller. The centrifugal pressure nozzle consists mainly of an internal nozzle channel, a filter to prevent orifice blocking (sintered metallic filter element, 10 µm), an O-ring to prevent water refrigerant from leaking outside the impeller, a swirl chamber for generating rotational flow, and an orifice for generating a thin liquid film. Water refrigerant pressurized by the centrifugal force of the impeller flows from the top part of the figure into the centrifugal pressure nozzle tangential to the swirl chamber, and then a thin liquid film is generated within the orifice by a turning force and sprayed. The sprayed liquid film is further ruptured, and fine particles are generated. The relationship between the pressure, spray droplet size and the flow rate was acquired from computational fluid dynamics (CFD) and nozzle unit tests using an external pressurization pump, realizing SMD 5.8 µm.

A 4.2 g/s spray requires 5 nozzles for each impeller. To suppress rotor unbalance, the nozzle arrangement on the shaft needs to be symmetrical. Because the nozzles are mounted between the blades, the number of nozzles that can be selected is the divisor of the number of impeller blades or the number obtained by subtracting the divisor from the number of blades. Because this needs to be considered when selecting the number of blades, prime numbers should be avoided. For example, if the first-stage impeller of this compressor has 15 blades, then the allowable number of nozzles is 3, 5, 10, 12, or 15.
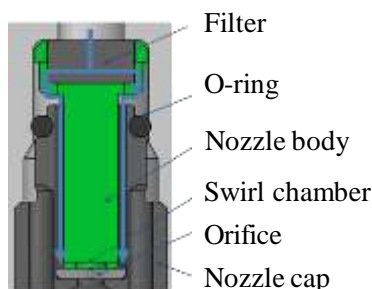

Figure 5: Centrifugal pressure nozzle configuration.

2.3 Condensing Ejector

The condensing ejector uses a high-speed fine refrigerant droplets to transfer momentum to the refrigerant vapor. And thus raises its pressure within a two-phase state. Figure 6 shows the exterior of the constructed 30RT condensing ejector. Because the spraying of refrigerant droplets using nozzles is necessary to limit the collision of refrigerant droplets with the wall surface of the mixing chamber, we require a spray form that conforms with the shape of the mixing chamber. Hence, we adopted a wall-impingement spray nozzle (Inamura et al., 2012). A wall-impingement spray nozzle consists of an impingement wall configured on concentric circles and multiple orifices for spraying water jets. The water jets impact the impingement wall, and thus form a liquid film. A fine droplet spray, which flies into

space, is then formed by liquid film instability. Because each spray flies out in a direction conforming to the impingement wall, it is possible to form a spray in any shape conforming to the shape of the mixing chamber. In the mixing chamber, momentum is transferred to refrigerant vapor from the high-speed fine refrigerant droplet spray, where vapor pressure is raised, and a differential is produced between the refrigerant droplet spray saturation pressure and the refrigerant vapor pressure. Thus, refrigerant vapor condenses into refrigerant droplets, and the vapor sucked into the condensing ejector is completely condensed at the outlet. That is, the vapor volume compressed by the condensing ejector is normally reduced compared to the compressor, and excess heat from the refrigerant vapor is constantly transferred to refrigerant droplets in the pressurization process, thereby significantly reducing the theoretical power.
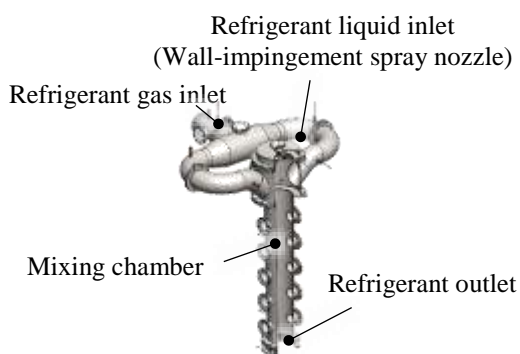

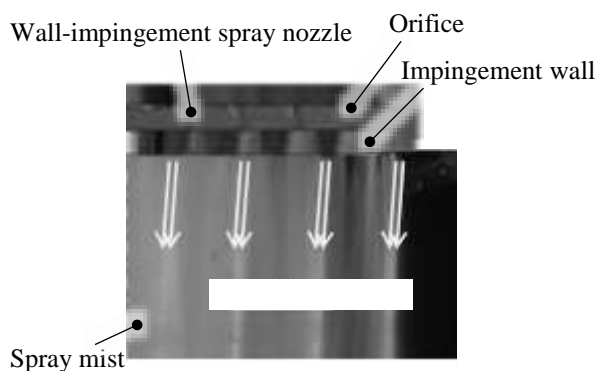**Figure 6:** 30RT Condensing Ejector.

Figure 7: Wall-impingement spray nozzle.

Figure 8 shows a schematic of a condensing ejector, and Fig. 9 shows a Mollier diagram. The condensing ejector consists of a wall-impingement spray nozzle (5) and a mixing chamber (2). Liquid refrigerant cooled by the plate heat exchanger (PHE) (4) is supplied to the wall-impingement spray nozzle (5) and then sprayed as fine, high-speed refrigerant droplets. In the mixing chamber (2), refrigerant vapor discharged by the continuous cooling compressor (1), and fine, high-speed refrigerant droplets sprayed from the wall-impingement spray nozzle (5) flow inside. Then, momentum is transferred to the refrigerant vapor from refrigerant droplets, where the refrigerant is compressed in a two-phase state. When this occurs, pressure rises in the mixing chamber with the refrigerant in a gas–liquid two-phase state, thus a pressure difference is produced between the saturation pressure of the sprayed liquid refrigerant and the pressure of the refrigerant vapor, and condensation occurs owing to the gas–liquid nonequilibrium. Consequently, the refrigerant vapor discharged from the continuous cooling compressor (1) completely condenses in the process of being compressed by the condensing ejector, and is discharged to a buffer tank (3) as liquid refrigerant. The PHE (4) consists of a heat dissipating circuit via a cooling tower, and it dissipates the heat condensed by the condensing ejector. The pressure ratio of the condensing ejector is determined by the temperature difference cooled by the PHE (4), and vapor is completely condensed in the process of being compressed by the condensing ejector at the 33.5 °C spray temperature of the wall-impingement spray nozzle (5) and the 38.5 °C condensing ejector discharge liquid refrigerant temperature; it is then discharged to the buffer tank ○as liquid refrigerant. If the PHE (4) temperature difference is 5 °C, then the pressure ratio reaches a maximum of 1.3. Table 3 shows the main specifications.
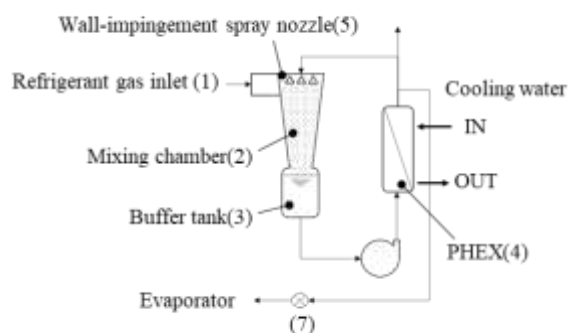

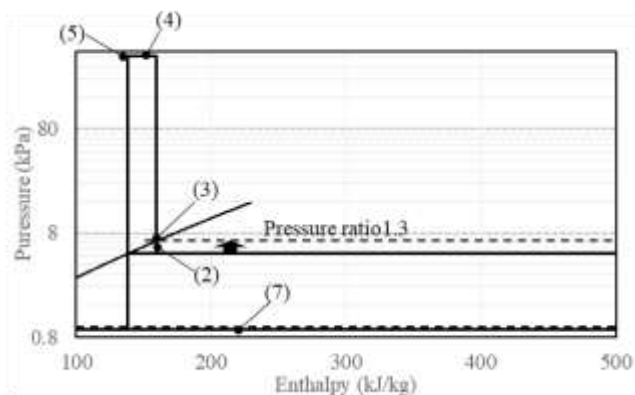**Figure 8:** Schematic of condensing ejector.

**Figure 9:** Mollier diagram of condensing process.

Table 3: Specification condensing ejector specification.

Ejector pressure ratio	1.30
Flow rate	300 [L/min]
External size (W × D × H)	Φ300 × 1700 [mm]
Spray pressure	200 [kPa]
Condensing capacity	120 [kW]

3. EXPERIMENTS

3.1 Refrigeration Cycle

To demonstrate the effects of a continuous cooling compressor and condensing ejector, we constructed a 30RT continuous cooling turbo chiller. Figure 10 shows a photograph of a continuous cooling turbo chiller. We demonstrated that a compression process that limits the degree of superheat can be realized using a continuous cooling compressor that sprays refrigerant droplets with a nozzles installed on impellers, and simultaneous compression and condensing can be realized with a condensing ejector that compressing vapor by refrigerant droplets. However, it was not possible to perform an evaluation using the rated pressure ratio owing to the insufficient pressure ratio of the condensing ejector. Realizing the target cycle performance requires the realization of a 1.3 pressure ratio by promoting atomization using the condensing ejector, and achieving power savings requires atomization using the centrifugal pressure nozzle of the continuous cooling turbo compressor. A COP of 4.86 can be expected with the former improvement, and a COP of 6.0 can be expected with the latter.
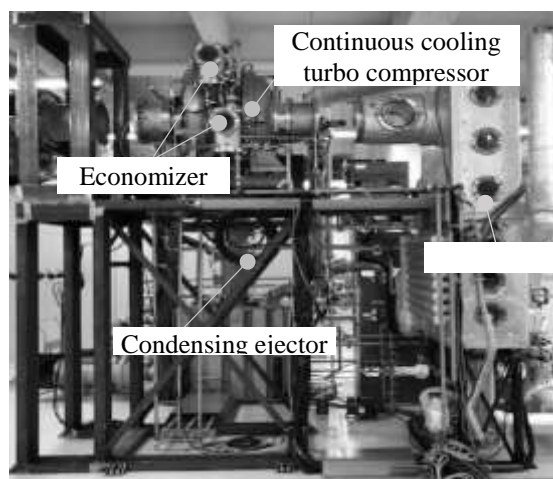
Figure 10: Continuous cooling turbo chiller.

3.2 Continuous Cooling Compressor

Here, we describe the experimental results for the spray flow rate and superheat of discharged refrigerant in continuous cooling compression. Cooling effects were insufficient and discharge superheat was 50 K with the 4.2 g/s spray flow rate of the 5 nozzles installed at each impeller of the initial design. To increase the cooling effect, nozzle installation holes were added between all of the blades. Rotor balancing was performed with plugs inserted with the same mass as the actual nozzles into the unused holes. Figure 11 shows the relationship between the total spray flow rate and the discharge superheat. When we mounted nozzles between all of the blades and increased the spray flow rate to 15.5 g/s, superheat of the discharged refrigerant vanished. The COP was less than when discharge superheat existed, but continuous cooling compression was demonstrated. The cause of the decrease in COP is assumed to be the reduced aerodynamic efficiency resulting from the increased spray flow rate. Furthermore, excess sprayed water flew out in large quantities from drain holes at the bottom of the volute. Therefore, we used 10, 8, and 7 nozzles for stages 1 to 3, respectively, to achieve a total spray flow rate of 6.9 g/s. Then the discharge superheat was 35 K, but shaft vibrations

during compressor operation were excessively large, and abnormal bearing wear was observed. The number of nozzles for the 3-stage impeller was not the divisor of 20 blades, and they were asymmetrically arranged. However, as described above, rotor balancing was performed by inserting plugs of equal mass. The cause of the unbalance is believed to have been sprayed water absent during balancing. This was present only on the asymmetrically arranged nozzles, which resulted in unbalance only during operation.

The spray flow rate required for continuous cooling compression with 0 K discharge superheat was 9.5 g/s. The cause of the increase from design values is considered to be an increased compressed vapor temperature due to decreased impeller adiabatic efficiency. The flow between the blades was analyzed and designed with CFD, accounting for the three dimensional blade shape. However, blockage due to droplets and the effects of continuous cooling were not considered in the analysis. The latter is considered to have little influence on the efficiency resulting from changes in the volumetric flow rate. With respect to the former, it is possible that the spray flow rate is increased due to coarse particles that does not contribute to the continuous cooling, which is inevitably included in particle diameter distribution. The channel area is blocked by the particles. Furthermore, the momentum transfer between the spray and vapor causes rapid deceleration of the compressed vapor flow, creating a large low-energy region. This results in the reduction of the actual flow area, causing a choke phenomenon. In addition, because water refrigerant has large viscosity, then a thick boundary layer is formed on the hub face of the impeller. The thickness would be increased by the spray droplets and form a large low-energy region. When designing a continuous cooling turbo impeller, such effects must be taken into consideration.
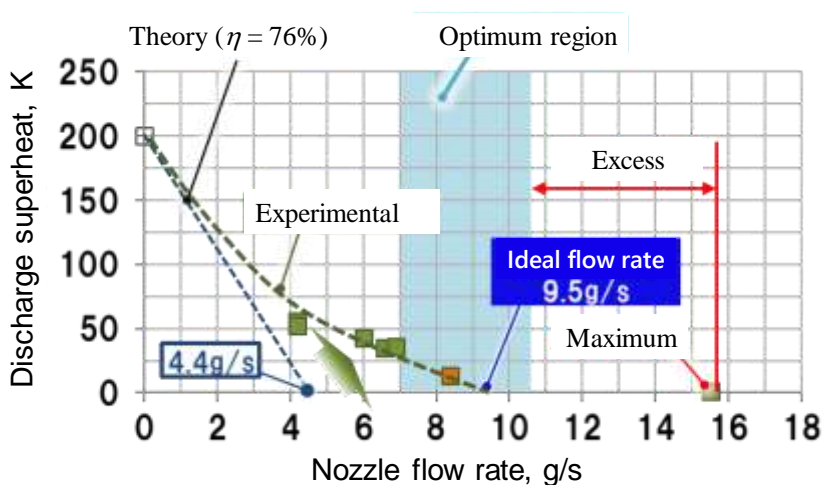

Figure 11: Discharge superheat and spray flow rate.

3.3 Condensing Ejector

Next, we describe the experimental results of the condensing ejector. Table 4 shows the pressurizing effects of the condensing ejector. The vapor that is sucked into the condensing ejector is pressurized at a pressure ratio of 1.11. The saturation temperature at a discharge vapor pressure of 3.16 kPa is 24.9 °C, which is in good agreement with the discharged refrigerant liquid temperature. Therefore, we demonstrated the basic principle of a condensing ejector, which compresses refrigerant vapor with the transfer of momentum from fine, high-speed droplets, allowing it to be pressurized in a two-phase state so that the vapor is completely condensed. However, the degree of pressurization was insufficient relative to the 1.3 design pressure ratio.

Table 4: Experimental result of condensing ejector.

Suction Vapor Pressure	2.84 kPa
Discharge Vapor pressure	3.16 kPa
Spray water Temperature	20.6 °C
Discharge water temperature	24.8 °C
Pressure ratio	1.11

Fluidity within the condensing ejector involves refrigerant droplets hovering about the refrigerant vapor at high speed. If the velocity of refrigerant droplets is faster than refrigerant vapor, then momentum is transferred to the refrigerant vapor. Thus, the refrigerant vapor pressure is increased, and condensing occurs owing to the gas–liquid nonequilibrium with refrigerant droplets. Formula (2) shows the amount of refrigerant vapor condensation S_{mas}, and Formula (3) shows the amount of momentum transferred to refrigerant vapor from refrigerant droplets per unit volume and unit time S_{mas}. Formula (4) shows the density of refrigerant droplets per unit volume.

$$S_{mas} = 0.23\rho_d 4\pi r^2 \rho_G a \left(\frac{P_G - P_{sat}(T_L)}{P_G}\right) \tag{2}$$

$$S_{mom} = -S_{mas}u_L + \rho_d 6\pi r \mu_G (u_L - u_G) \tag{3}$$

$$\rho_d = \frac{3M_L}{4\pi r^3}\frac{1}{Au_L} \tag{4}$$

The condensing of refrigerant vapor is produced by the difference between the saturation pressure of droplet $P_{sat}(T_L)$ and refrigerant vapor pressure P_G at the refrigerant droplet temperature. Momentum transfer is produced by the transfer owing to condensation, as well as the difference between the refrigerant droplet velocity u_L and refrigerant vapor flow rate u_G. This transfer increases as the refrigerant droplet radius r decreases. Consequently, the large particle size of the refrigerant droplets causes an insufficient momentum transfer, resulting in an insufficient pressure increase compared to the design pressure ratio of 1.3.

4. CONCLUSIONS

- The continuous cooling turbo chiller equipped with a continuous cooling compressor and condensing ejector was constructed to demonstrate the basic principle of each element.
- Realizing the target COP requires the further atomization of refrigerant droplets sprayed by the centrifugal pressure nozzle of the continuous cooling compressor and wall-impingement spray nozzle of the condensing ejector. A COP of 4.86 could be expected by promoting atomization by the wall-impingement spray nozzle, and a COP of 6.0 could be expected by promoting atomization by the centrifugal pressure nozzle.
- Suppression of discharge superheat was demonstrated by the continuous cooling compression technology that sprays centrifugally pressurized water refrigerant from a impeller
- The impeller efficiency is diminished by the blockage effect of unevaporated residual droplets, which decreases the COP. Designing the aerodynamics of impellers requires some consideration of the effects of spray droplets as well.
- The basic principle of a condensing ejector was demonstrated. The condensing ejector uses a high-speed fine refrigerant droplets to transfer momentum to the refrigerant vapor. And thus raises its pressure within a two-phase state and simultaneously condensing refrigerant vapor.
- Momentum transfer is achieved by the difference between the refrigerant droplet velocity u_L and the refrigerant vapor velocity u_G, in addition to the volume of refrigerant transferred by condensing, and it increases as the refrigerant droplet radius r becomes smaller. Realizing the design pressure ratio requires the construction of a nozzle that sprays even finer refrigerant droplets.

NOMENCLATURE

ρ_d	droplet density	kg/m^3
r	radius of droplet	m
ρ	density	kg/m^3
a	sonic speed	m/s
P	pressure	Pa
u	velocity	m/s
μ	viscosity	Pa · s
M	volume flow rate	m^3/s
A	cross section area	m^2

Subscript

G	gas
L	liquid
sat	saturation

REFERENCES

Kilicarslan A, & Müller N. (2005). A Comparative Study of Water as a Refrigerant with Some Current Refrigerants. Int. J. Energy Res, *29*(11), 947–959.

Shoyama, T., Kawano, B., Ogata, T., Matsui, M., Furukawa, M., & Dousti, S. (2020). Centrifugal Turbo Chiller Using Water as Refrigerant and Lubricant. *J. Proc. Mech. Eng.*, 0954408920938197.

Wu, H., Yin, H., Li, Y., & Xu, X. (2019). Effect of Droplets on Water Vapor Compression Performance. *Desalin.*, *464*, 33–47.

Inamura, T., Yanaoka, H., & Tomoda, T. (2012). Prediction of Mean Droplet Size of Sprays Issued from Wall Impingement Injector. *AIAA Journal*, *42*(3), 614–621.

Marble, F. E. (1968). Some Gasdynamic Problems in the Flow of Condensing Vapors. *Acta Astronautica*, *14*, 585–614.

ACKNOWLEDGEMENT